# Experimental Investigation of Radiation Emitted by Optically Thin to Optically Thick Wildland Flames

P. Boulet, B Porterie, A. Kaiss

Hindawi Publishing Corporation
Journal of Combustion
Volume 2011, Article ID 137437, 8 pages
doi:10.1155/2011/137437

*Research Article*

# Experimental Investigation of Radiation Emitted by Optically Thin to Optically Thick Wildland Flames

**P. Boulet,[1] G. Parent,[1] Z. Acem,[1] A. Kaiss,[2] Y. Billaud,[2] B. Porterie,[2] Y. Pizzo,[2,3] and C. Picard[3]**

[1] *LEMTA, Nancy-Université, CNRS, Faculté des Sciences et Technologies, BP 70239, 54506 Vandœuvre Cedex, France*
[2] *IUSTI/UMR CNRS 6595, Université de Provence, 5 rue Enrico Fermi, 13453 Marseille Cedex 13, France*
[3] *CEREN, Domaine de Valabre, 13120 Gardanne, France*

Correspondence should be addressed to P. Boulet, pascal.boulet@lemta.uhp-nancy.fr

Received 30 December 2010; Accepted 15 February 2011

Academic Editor: Paul-Antoine Santoni



A series of outdoor experiments were conducted in a fire tunnel to measure the emission of infrared radiation from wildland flames, using a FTIR spectrometer combined with a multispectral camera. Flames of different sizes were produced by the combustion of vegetation sets close to wildland fuel beds, using wood shavings and kermes oak shrubs as fuels. The nongray radiation of the gas-soot mixture was clearly observed from the infrared emitted intensities. It was found that the flame resulting from the combustion of the 0.50 m long fuel bed, with a near-zero soot emission, may be considered as optically thin and that the increase in bed length, from 1 to 4 m, led to an increase in flame thickness, and therefore, in flame emission with contributions from both soot and gases. A further analysis of the emission was conducted in order to evaluate effective flame properties (i.e., emissivity, extinction coefficient, and temperature). The observation of emission spectra suggests thermal nonequilibrium between soot particles and gas species that can be attributed to the presence of relatively cold soot and hot gases within the flame.

## 1. Introduction

Radiation heat transfer plays an important role in the ignition, spread, and intensity of wildland fires. The experimental characterization of radiation from wildland flames is a very active field of research, as demonstrated by recent contributions (e.g., Chetehouna et al. [1], Butler et al. [2], Dupuy et al. [3], Boulet et al. [4], Agueda et al. [5], and Parent et al. [6]). These contributions raise some important issues, such as those related to the uncertainties and interpretation of results and to the importance of flame scale.

A commonly used simplified approach consists in evaluating effective flame properties, modeling the flame as a radiating surface with constant temperature and emissivity. However, neglecting the distributions of temperature and species concentrations and the wavelength dependence and ignoring that emission comes from the volume of flame (or a part of it) can cause noticeable errors. Moreover, temperature and emissivity are two unknowns that must be determined from a single emission acquisition. An alternative approach to estimating flame emission is to determine an extinction coefficient that includes the contributions of both gas species and soot and to consider radiation coming from a volumetric domain representing the flame.

When dealing with radiation measurements, special attention to the spectral range is required. Water vapor is known to produce emission bands in the ranges [5–8 $\mu$m] and [2.5–3 $\mu$m] (see Boulet et al. [4]), whereas the main emission band of carbon products is around 4.3 $\mu$m approximately, and soot emits radiation in a continuous spectrum over the infrared region. The near- to mid-infrared range has therefore to be considered for accurate measurements of soot and gas emission. Using a device that collects emission data in a too narrow or inappropriate spectral range may lead to uncertain conclusions.

The optical thickness of the flame is known to be a crucial parameter in the investigation of radiation emission. For laboratory flames involved in a previous contribution [4], the emission from the gas band was evident and the continuous soot emission was hardly found. This behavior was related to the optically thin nature of the flame due to its small size

and to a low soot production resulting from an efficient (i.e., well-oxygenated) combustion. In the present investigation, a campaign of measurements is conducted with the aim of evaluating the spectral emission from flames of increasing sizes. Data collected from experimental fires performed in the CEREN's fire tunnel in July 2010 are analyzed and used to evaluate effective flame properties. Considering this paper as a preliminary study of the experimental characterization of radiation from wildland flames, wood shaving and kermes oak shrubs are used as two approximations to actual fuel beds.

## 2. Experimental Setup

The experimental setup that was used and described extensively in a previous work [6] included a FTIR spectrometer (MATRIX by Bruker) and a classical IR camera with external spectral filters that had to be changed by hand. A silicon beam splitter divides the signal into two separate signals; one is transmitted to the IR camera and the other to the spectrometer. For the present experimental campaign, the only modification to the original setup was the replacement of the classical IR camera with a multispectral camera, the spectral bands being selected by filters mounted on a rotating filter wheel, with a filter transition time of approximately 40 ms. The main advantage of the new setup is that measurements for 3 definite spectral bands along with the total integrated signal can be obtained from a single experimental run. This avoids the problem of successive runs with manually changed filters, which reduces repeatability concerns to acceptable levels. The multispectral camera has a range of sensitivity of 1.5–5 $\mu$m, which allows the observation of a large part of the spectral emission pattern of combustion products. A broader spectral range may be obtained with the spectrometer, since its MCT/InSb dual detector operates over the wavelength range of 1.6–10 $\mu$m.

The filters of the multispectral camera were selected according to the infrared spectral emission bands of the main combustion products:

(i) a filter in the range of 2.8–2.9 $\mu$m for $H_2O$,

(ii) a filter in the range of 4.24–4.26 $\mu$m for CO and $CO_2$,

(iii) a filter in the range of 3.88–3.92 $\mu$m for soot, apart from the emission bands of $H_2O$, CO, and $CO_2$,

(iv) a 1% transmission filter in the whole range of the camera (i.e., 1.5–5 $\mu$m).

Prior to measurements, the camera was calibrated with a black-body radiation source. In a previous work [6], details of the calibration procedure are given and some sensitivity and repeatability aspects are discussed.

Two series of experiments were carried out by the authors in the fire tunnel of the CEREN (Figure 1). The overall dimensions of the tunnel are 2.75 m high, 2.4 m wide, and 8 m in length. The lower part of the tunnel sidewalls is made of cellular concrete, wire mesh completing the upper part of the walls and the ceiling to prevent firebrand ejection. The ends of the tunnel are open. Two types of fuels were used: wood shavings (hereafter called WS) and kermes oak (*Quercus coccifera*) shrubs (hereafter called KO). Fuel bed properties are given in Table 1. The fuel to be burned was distributed uniformly on a combustion platform with a 1 m width and a length varying from 0.5 to 4 m in such a manner that the load and height of the layer were the same whatever the bed length. In the first series of experiments, the only fuel was wood shavings. It was arranged to give a layer of uniform load of 1 kg/m$^2$ and of 0.1 m height. In the second series, both WS and KO were used as fuels. KO items were evenly spaced and vertically arranged in the most stable position to form a 1 m high homogenous layer. Wood shavings were used as litter with a height of 0.2 m. Fuel loads of WS and KO were estimated at 2 kg/m$^2$ and 9 kg/m$^2$, respectively.

Table 1: Properties of the test fuel beds considered in this study.

| | Load (kg/m$^2$) | Bulk density (kg/m$^3$) | Surface-to-volume ratio (m$^{-1}$) | Fuel moisture content |
|---|---|---|---|---|
| Kermes oak shrubs | 9 | 480[a] | 5950 | 40.1 |
| Wood shavings | 2 | 630[a] | 1500 | 10.0 |

[a] Present work.

In order to produce fuel bed combustion as homogeneous as possible, the ignition was done at different locations using hand-held gas burners. The use of a liquid hydrocarbon fuel was dismissed since its combustion may generate products that may have undesirable effects on the spectral emission. The ignition phase lasted only a few seconds, after which successive measurements were done simultaneously by the spectrometer and by the camera. Data were collected continuously throughout the period of flaming combustion (i.e., as long as the visible flame was present), typically from a few tens of seconds for the 0.50 m long WS bed to up to 2 minutes for the 4 m long KO bed. Measurements were made 20 cm above the top of the vegetation.

Depending on the flaming combustion duration, up to 10 acquisitions were registered for each run, in order to determine how fire emission changes over time. Moreover, data obtained at the moment of maximum emission allows a comparative analysis between the IR spectra and images from WS and KO flames of different sizes.

A total of 22 fires were conducted with varying fuel bed lengths and vegetation types.

## 3. Flame Emission Spectra

Figure 2(a) shows the spectral intensity as a function of wavenumber and wavelength at five different instants during the burning of the 1-m-long WS fuel bed. The time evolution of the intensity integrated over the wavenumbers, shown in Figure 2(b), is deduced from six successive acquisitions during the run. In this diagram, flame emission increases rapidly to reach a maximum value of 25 kW/m$^2\cdot$sr approximately 12 s after ignition. Then it decreases, with some unavoidable

(a) (b)

Figure 1: Photographs of the experimental setup showing the arrangement of the 3 m × 1 m wood shaving fuel bed (a) and of a typical test where kermes oak shrubs were burning (b). The spectrometer is on the foreground.

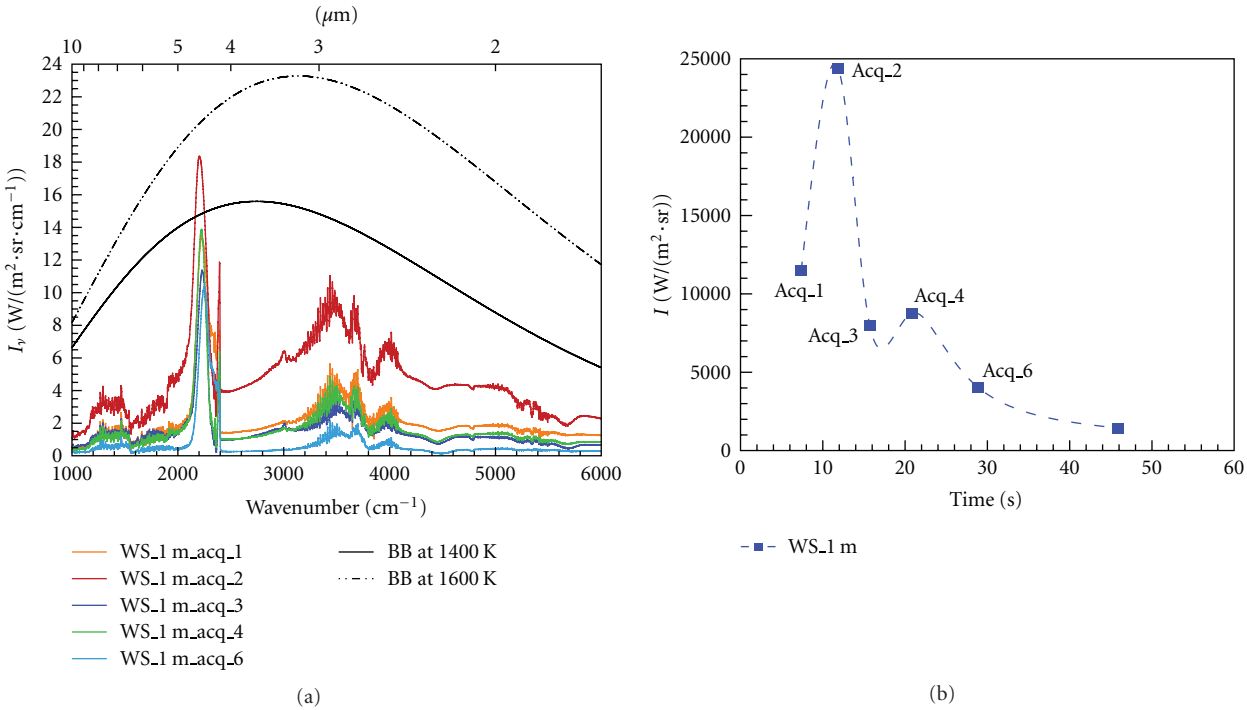


(a) (b)

Figure 2: Emitted radiation from flames generated by the burning of the 1 m long WS fuel bed. (a) Spectral intensity versus wavenumber (and wavelength) obtained from successive acquisitions and (b) intensity integrated over wavenumber versus time. Solid and dotted black lines correspond to blackbody emission curves at temperatures of 1400 K and 1600 K. The fuel load is 1 kg/m$^2$.

variations due to flame flickering. Easily recognizable peaks in the IR spectra (Figure 2(a)) are those due to hot $CO_2$ and CO molecules, at around 2300 cm$^{-1}$ (4.3 $\mu$m), and the others due to water vapor in the combustion products. Some signal variations are found to be in agreement with those obtained for thin flames (e.g., Boulet et al. [4] and Parent et al. [6] for vegetation fires and Bourayou et al. [7] for small burner flames). Unlike these studies, the emission spectra show, aside from these peaks, a continuum radiation from glowing soot particles in the flame. This is clearly visible in Figure 2(a) from acquisition 2, which corresponds to the time at which emission is maximum. A crude estimation of the maximum emission level may be provided by plotting the blackbody emission curves at somewhat arbitrary temperatures, here 1400 K and 1600 K. It can be observed that, around the 2300 cm$^{-1}$ peak, the maximum flame emission is in between, indicating that the flame temperature must be in the range of 1400 K–1600 K. On the contrary, the emission is lower in the spectral ranges where emission is originating from soot and water

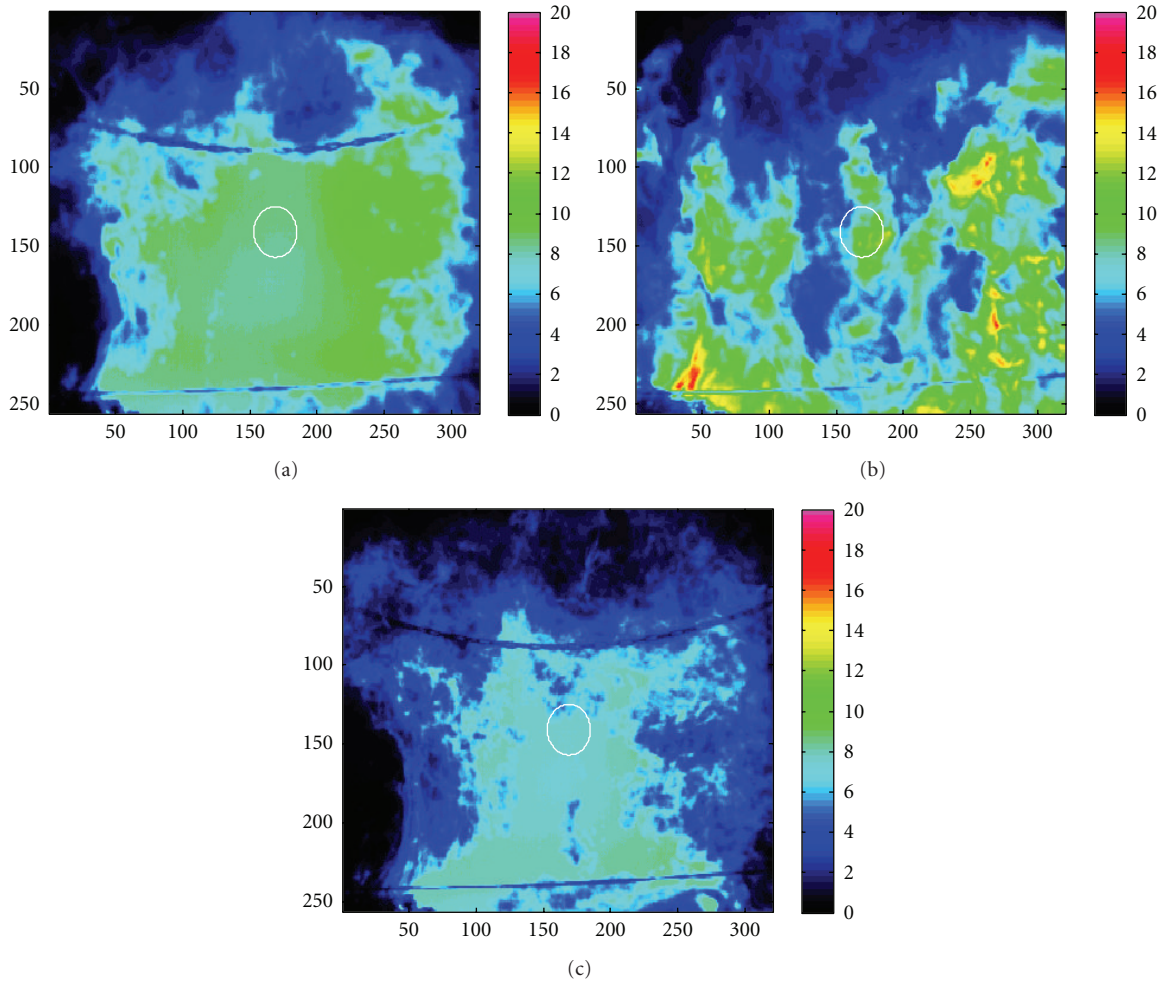


FIGURE 3: Flames generated by the burning of the 2 m long WS fuel bed: camera acquisitions in the emission bands of $CO_2$ (a), $H_2O$ (b), and soot (c). Color bar indicates spectral intensity in $W/m^2 \cdot sr \cdot cm^{-1}$. The white circle delimits the observation area of the spectrometer. The fuel load is 1 $kg/m^2$.

vapor, indicating either a lower emissivity and/or a lower temperature. These results are obtained for a 1 m long flame that cannot be considered as optically thick.

Spectral emission intensity may also be estimated from camera acquisitions in the infrared emission bands where $CO_2$, $H_2O$, or soot radiation is dominant. An example is given in Figure 3 for the flaming combustion of the 2 m long WS fuel bed. The time interval between two successive acquisitions is 40 ms (i.e., filter change time). This means that the multispectral camera is capable of acquiring quasisimultaneous images, which makes it very attractive.

First of all, the aforementioned trend is confirmed, namely, a strong emission of gaseous species, with a relevant contribution from inflame soot particles. Figure 3 also reveals heterogeneities in the structure of the flame as a consequence of variations in species concentrations and temperature.

As mentioned before, the emission intensities provided by the spectrometer in the range of 1.6–10 $\mu$m correspond to spectral intensities spatially averaged over a small area of the flame region (Figure 3), approximately 25 $cm^2$ at two meters from the spectrometer. Although not shown, these data are in qualitative agreement with the multispectral camera measurements.

Figure 4 represents the maximum emission spectra obtained from the burning of WS fuel beds with a length varying from 0.50 to 4 m (e.g., Acq_2 in Figure 2 is the maximum emission spectra for the 1 m long flame in Figure 4). In this figure, spectral intensities are plotted as a function of wavenumber and wavelength. It is easy to observe that the emission level increases with the fuel bed length. A discriminant analysis shows that the emitted intensity around 2300 $cm^{-1}$ ($CO_2$ products) seems to saturate, indicating that the opaque limit has been reached in this spectral range. This is not the case for the rest of the spectrum where the emitted intensities are still rising between 3 m and 4 m. In any case, the role of soot in radiation emission is evident. The near-zero emission level aside from the gas peaks for the 0.5 m long fuel bed is characteristic of an optically-thin flame. This is consistent with the conclusion drawn from

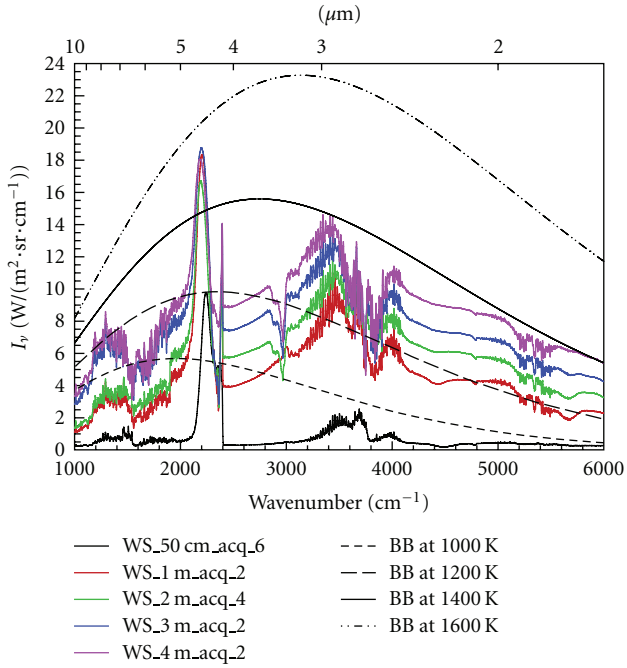


Figure 4: Maximum emission spectra from WS fuel beds with a length varying from 0.5 to 4 m. The fuel bed load is 1 kg/m$^2$. Typical blackbody emission curves are plotted for the comparison.

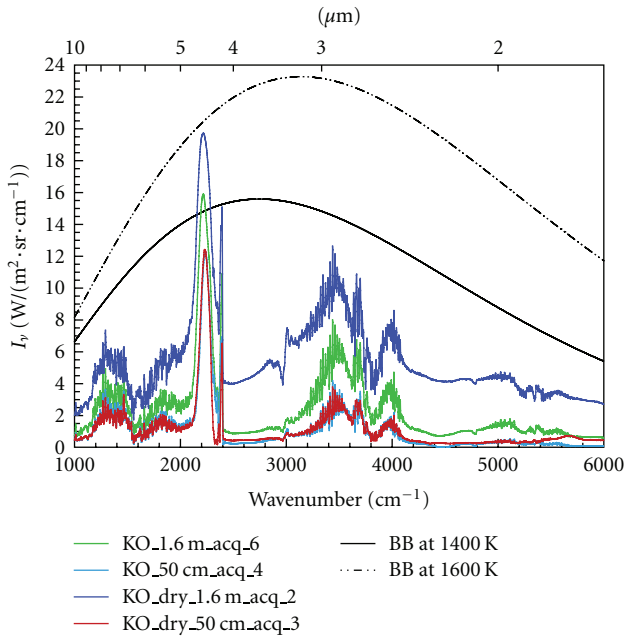


Figure 5: Maximum emission spectra for KO fuel beds of various lengths. The fuel load is 9 kg/m$^2$.

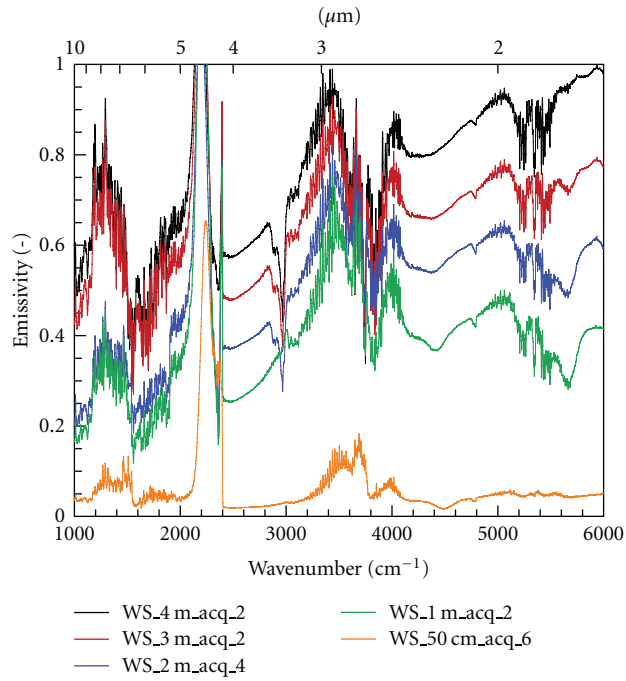


Figure 6: Emissivity computed from maximum emission spectra versus wavenumber (and wavelength). WS are used as fuel, with a fuel load of 1 kg/m$^2$.

a previous study [4]. For flame lengths greater than 0.5 m, radiation emission becomes relevant in the whole infrared range, as may be easily deduced from the comparison with blackbody emission curves for temperatures of 1000, 1200, 1400, and 1600 K. From the spectral shape of flame emissions (Figure 4), it may be stated that the flame emissivity is stronger for large wavenumbers (in this range, emission spectra are closer to blackbody spectra) and that the emission level decreases for small wavenumbers. This is in agreement with the expectation that the absorption coefficient of soot strongly rises with wavenumber, as it will be discussed below. If the assumption of opaque flame holds for large wavenumbers, one can observe that the 4 m long flame emission starts from that of a blackbody at 1400 K, defining an effective flame temperature. However, this assumption is questionable for at least two reasons. First, the emission intensities still vary for the 3 m- and 4 m long flames. Second, a higher emission level is reached in the range attributed to $CO_2$ emission. This shows that the so-called effective temperature is overwhelmed (emissivity cannot be greater than unity) and that the gas temperature should be close to 1600 K.

Concerning the opacity of the flame, it is customary to assume that the absorption coefficient of soot varies with wavelength as $1/\lambda^a$ [8]. The dispersion exponent $a$ is an empirical constant, ranging from 0.7 to 2.2, depending on the chemical composition and the porosity of soot particles. The identification of these properties is beyond the scope of the present study, but a $1/\lambda$ wavelength dependence is often considered as a good approximation [8]. This means that the greatest absorption coefficients are at the smallest wavelengths (or at the greatest wavenumbers, approximately in the range of [5600–6000 cm$^{-1}$]), giving some justification to the assumption of blackbody emission in this range and some confidence in the reference value of 1400 K for the flame temperature. Therefore, considering the emission above, the 1400 K blackbody spectrum in the

range attributed to CO–$CO_2$, this suggests the presence of large quantities of relatively cold soot within the flame. This was already observed by Sivathanu et al. [9] for strongly radiating jet flames, and by Suo-Anttila et al. [10] for ethanol, ethanol/toluene, JP8, and heptane pool fires. The maximum emission observed in Figure 4 is between the blackbody emission curves at 1400 and 1600 K and corresponds to the emission of a blackbody at a temperature of 1522 K. This temperature may be interpreted as the gas temperature.

A similar experimental study was carried out using KO as fuel. Figure 5 shows the maximum emission spectra obtained from the burning of KO fuel beds with a length ranging from 0.5 to 3 m. Data for fresh and dry KO are reported for the same load and same flame length. The comparison between Figures 4 and 5 indicates that the change in fuel type significantly affects flame emission. As previously observed for WS fuel beds, the trend of an increasing emission with fuel bed length is also seen, but with lower emission levels. The emission from soot is also undoubtedly observed. The emission at around 2300 $cm^{-1}$ is still very high, close to that of a blackbody at 1600 K. Emission spectra obtained using fresh KO as fuel gave lower intensities from both inflame soot particles and gas species, as a consequence of different thermal degradation processes.

## 4. Spectral Radiative Properties

The spectral emitted intensity may be evaluated from the spectral blackbody intensity as

$$I_\nu = \varepsilon_\nu I_\nu^0. \tag{1}$$

The emissivity $\varepsilon_\nu$ can be related to the extinction coefficient $K_\nu$ and the flame thickness $L$ as

$$\varepsilon_\nu = 1 - e^{-K_\nu L}. \tag{2}$$

The blackbody intensity is computed as (Modest [8])

$$I_\nu^0 = \frac{2hc_0^2\nu^3}{n^2}\left[\exp\left(\frac{hc_0\nu}{nkT}\right) - 1\right]^{-1}, \tag{3}$$

where $h$ is the Planck's constant, $c_0$ is the celerity of light in vacuum, $\nu$ is the wavenumber, $n$ is the refraction index of the medium (here, $n = 1$), $k$ is the Boltzmann's constant, and $T$ is the temperature.

One can proceed to an identification of the above parameters $\varepsilon_\nu$ and $K_\nu$ using the data acquired for various fuel bed lengths. Typical results are commented below.

Assuming an effective flame temperature of 1400 K, neglecting the surrounding emission, and using the data reported in Figure 4, a spectral emissivity is first deduced from relation (1). Results are plotted in Figure 6 for WS fuel beds. In a logical manner, the emissivity increases with the bed length as a consequence of an increasing optical thickness due to the enhancement of the soot contribution. The lowest emission is obtained from the burning of the 0.50 m long fuel bed. The flame generated is optically thin, and its emissivity is relevant only in the gas emission bands. For thicker flames, the emissivity is greater in the whole spectral range considered. For a given flame thickness, the trend shows an increase in the emissivity with the wavenumber (as expected since soot absorption increases with wavenumber). A clear drawback of the present method based on a reference temperature is that the so-called emissivity seems to increase above unity in the range near 2300 $cm^{-1}$. The problem was expected since the emission of the flame is above the one of the blackbody at 1400 K (Figure 4). Once again, this raises the problem of defining an effective temperature, with soot and gas species in thermal nonequilibrium within the flame. However, we decided to go further in the analysis by trying to identify an extinction coefficient as a function of the wavenumber. Inverting relation (2) gives

$$K_\nu = \frac{-1}{L}\ln(1 - \varepsilon_\nu). \tag{4}$$

Assuming that the extinction coefficient is an intrinsic property of vegetation, this relation should provide a unique value of $K_\nu$. As shown in Figure 7(a), the burning of the shortest fuel bed (i.e., 0.5 m) generates a flame with a significantly lower extinction coefficient than the others. A possible explanation could be that less inflame soot is produced due to a more complete combustion. A spectral extinction coefficient independent of the fuel bed length may be determined by averaging the extinction coefficients of each fuel bed length (Figure 7(b)). The extinction coefficient varies between 0.1 and 1.0, which is in agreement with the literature (see the review by Agueda et al. [5]). A strong spectral dependency is observed. Note that the area around the $CO_2$ peak has been cut-off in order to avoid unphysical results. It is worth reminding that the atmospheric gases are partly absorbing radiation emitted from the flame, which affects extinction in some definite bands. Atmospheric water vapor and carbon dioxide absorb radiation in some parts of the IR region that are not exactly the same than the emission bands of hot $H_20$ and $CO_2$ produced by the flame. This explains the strong decrease down to 0.1 $m^{-1}$ in the extinction coefficient at about 2300 $cm^{-1}$, due to the atmospheric $CO_2$ absorption (Figure 7(b)). The same behavior is observed in the bands of water vapor.

## 5. Effective Radiative Properties

Despite the large spectral variations, effective values may be computed by integrating the data over wavenumber. This can provide useful input data for nonspectral radiation models such as the emissivity, the extinction coefficient, and the temperature. For the fuel bed lengths considered, the effective intensity is computed between 1000 and 6000 $cm^{-1}$ and divided by the blackbody emission intensity at an arbitrary temperature, here 1400 K. Effective values are summarized in Table 2. As the fuel bed length increases from 1 m to 4 m, the effective intensity increases from 4.2 to 43 $kW/m^2 \cdot sr$ and the so-called emissivity from 0.41 to 0.74. The average extinction coefficient obtained by inverting relation (2) yields values in the range of 0.34–0.53, with an average value of 0.40 $m^{-1}$. As aforementioned, the higher value determined for the 1 m long fuel bed is probably a consequence of flame flickering effects. Table 2 shows that

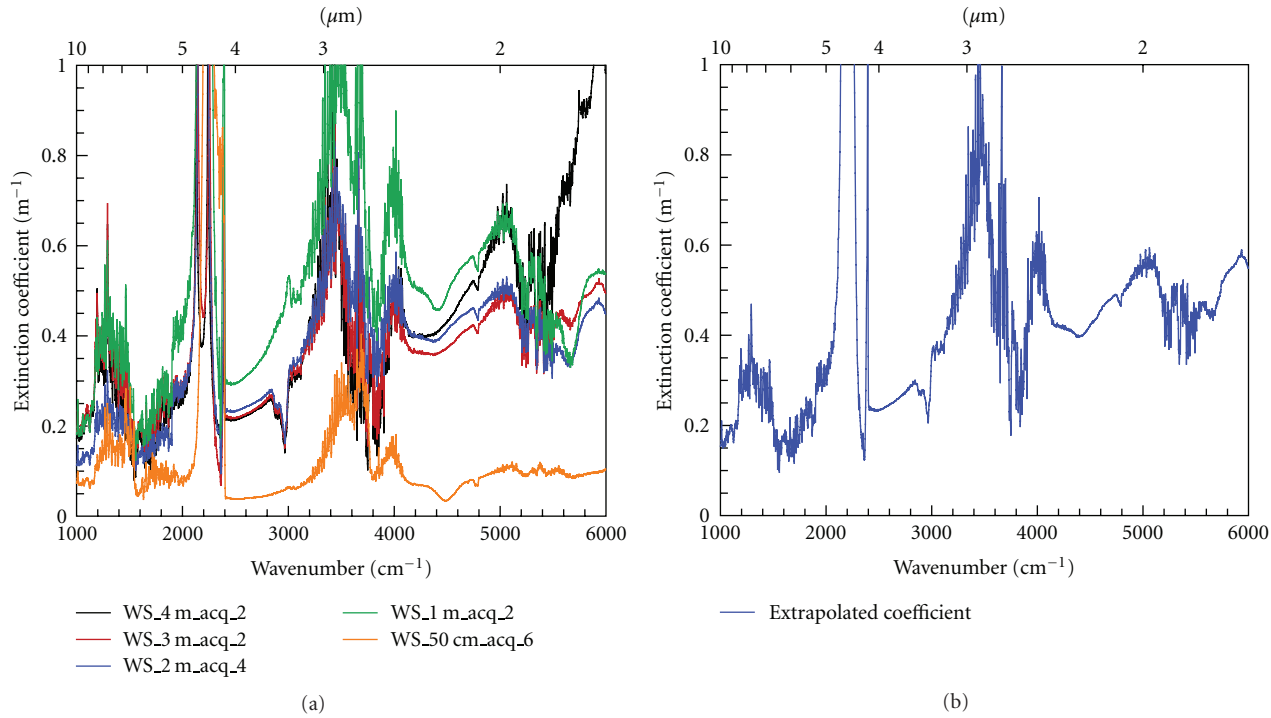


Figure 7: (a) Extinction coefficient versus wavenumber (and wavelength) and (b) averaged extinction coefficient versus wavenumber (and wavelength). WS are used as fuel, with a fuel load of 1 kg/m$^2$.

Table 2: Effective radiative properties of the flame. WS are used as fuel, with a fuel load of 1 kg/m$^2$.

| Fuel bed length | 0.5 m | 1 m | 2 m | 3 m | 4 m |
|---|---|---|---|---|---|
| Effective intensity I (kW/m$^2$·sr) | 4.2 | 23.8 | 29.7 | 37.8 | 43.4 |
| $\varepsilon = I/I^0$ (1400 K) | 0.07 | 0.41 | 0.51 | 0.65 | 0.74 |
| Mean extinction coefficient $\kappa$ (m$^{-1}$) | 0.15 | 0.53 | 0.36 | 0.35 | 0.34 |

the extinction coefficients are nearly the same for bed lengths greater or equal to 2 m; beyond, this coefficient seems to be a constant radiative property of the flame. It is also worth noting that the optically thin flame resulting from the combustion of the 0.50 m long fuel bed, with a near-zero soot emission, is characterized by significantly lower effective values.

Although not shown, the same analysis has been performed using dry KO as fuel, leading to an effective intensity of 27.5 kW/m$^2$·sr, an emissivity of 0.47, and an average extinction coefficient of 0.40 m$^{-1}$.

## 6. Emission from the Burning Fuel Bed

Experiments were also conducted to investigate the emission coming from the burning fuel bed. The spectrometer was inclined with an angle close to 10° in order to modify the line of sight. A thickness of flame around 1m is crossed by the line of sight of the acquisition device. Radiation came not only from the flame, but also from the burning embers at the basis of the flame (called hereafter the "burning litter"). This additional emission is partly absorbed by the flame, but as 1 m long flame is not totally opaque, some emission was expected to come from the hot burning embers. Typical emission results are presented in Figure 8 for WS fuel beds. Apart from the gas emission, a strong continuous emission is now observed that comes from both the soot and the burning vegetation. A comparison with the spectra of the 1 m long flame (Figure 4) shows that the emission levels are quite unchanged in the high wavenumber range, whereas some discrepancies appear for small wavenumbers. One can observe that the emission level is slightly higher on Figure 8 due to the emission from the burning litter. As a consequence, a slightly different continuous pattern was seen, with a higher emission in the small wavenumbers, that is, in the range where soot emission starts to decrease. This observation confirms that the contribution of the burning litter to the radiative heat transfer must be considered, as it was previously reported in [4], especially in the case of optically-thin flames, for which a weak continuous emission from soot was observed.

## 7. Concluding Remarks

Infrared radiation emitted from flames during the combustion of wildland fuel beds was investigated. Fuel beds of different lengths were considered, leading to both optically thin and optically thick flames. Both gas band radiation and continuous soot radiation were evident. A strong wavelength dependence of the emission spectra was observed,

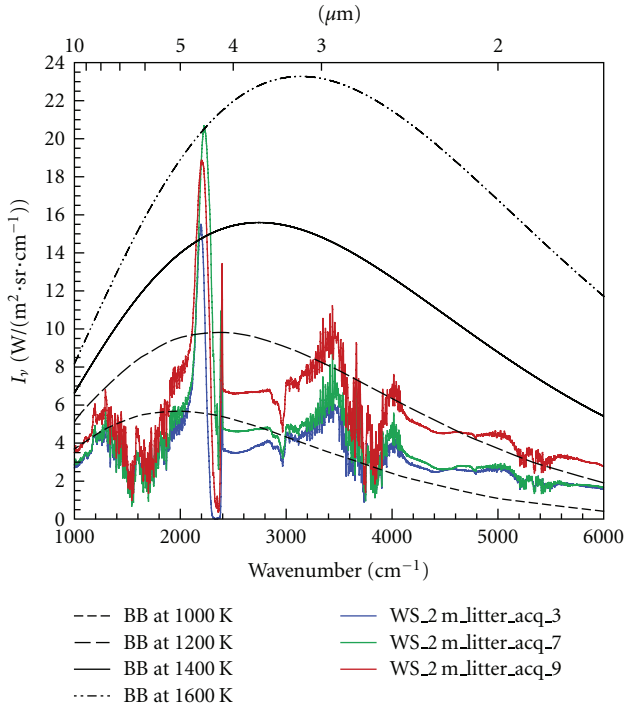


Figure 8: Emission spectra resulting from the burning of the 2 m long WS fuel bed, with a line of sight coming from the burning litter. The fuel load is 1 kg/m$^2$.

which confirms the requirement of devices with extended sensitivity ranges for the measurement of spectral radiation intensities from wildfires. Spectral and effective radiative properties were proposed. Effective emissivities from 0.41 to 0.74 were found for flames of length ranging from 1 to 4 m. A comparative analysis of the emission over different wavelength ranges suggests the coexistence of relatively cold soot and hot gases within the flame. The problem of assuming an effective temperature, with soot and gas species in thermal equilibrium, was therefore addressed. An optimization method based on a genetic algorithm and spectral radiation models for the soot and the gaseous combustion products is in progress in order to identify in a more accurate manner the respective temperature levels and the volume fractions of soot and gas species. Despite the information gained with the present study on emission levels, further treatment of the camera acquisitions is required in order to correlate emitted intensity with flame fluctuations.

## Nomenclature

$c_0$: Celerity of light in vacuum (m·s$^{-1}$)
$h$: Planck's constant (J·s)
$I_\nu$: Intensity (W·m$^{-2}$·sr$^{-1}$/cm$^{-1}$)
$k$: Boltzmann's constant (J·K$^{-1}$)
$K$: Extinction coefficient (m$^{-1}$)
$L$: Flame length (m)
$n$: Refraction index (−)
$T$: Temperature (K).

## Greek Letters and Abbreviations

$\varepsilon$: emissivity (-)
$\lambda$: Wavelength ($\mu$m)
$\nu$: Wavenumber (cm$^{-1}$), spectral property
FTIR: Fourier transform infraRed
KO: Kermes oak
WS: Wood shaving.

## References

[1] K. Chetehouna, O. Séro-Guillaume, and A. Degiovanni, "Measurement of radiative absorption coefficient for a vegetal medium," *Measurement Science and Technology*, vol. 15, no. 6, pp. N43–N46, 2004.

[2] B. W. Butler, J. Cohen, D. J. Latham et al., "Measurements of radiant emissive power and temperatures in crown fires," *Canadian Journal of Forest Research*, vol. 34, no. 8, pp. 1577–1587, 2004.

[3] J. L. Dupuy, P. Vachet, J. Maréchal, J. Meléndez, and A. J. De Castro, "Thermal infrared emissiontransmission measurements in flames from a cylindrical forest fuel burner," *International Journal of Wildland Fire*, vol. 16, no. 3, pp. 324–340, 2007.

[4] P. Boulet, G. Parent, A. Collin et al., "Spectral emission of flames from laboratory-scale vegetation fires," *International Journal of Wildland Fire*, vol. 18, no. 7, pp. 875–884, 2009.

[5] A. Agueda, E. Pastor, Y. Pérez, and E. Planas, "Experimental study of the emissivity of flames resulting from the combustion of forest fuels," *International Journal of Thermal Sciences*, vol. 49, no. 3, pp. 543–554, 2010.

[6] G. Parent, Z. Acem, S. Lechêne, and P. Boulet, "Measurement of infrared radiation emitted by the flame of a vegetation fire," *International Journal of Thermal Sciences*, vol. 49, no. 3, pp. 555–562, 2010.

[7] R. Bourayou, R. Vaillon, and J.-F. Sacadura, "FTIR low resolution emission spectrometry of a laboratory-scale diffusion flame: experimental set-up," *Experimental Thermal and Fluid Science*, vol. 26, no. 2-4, pp. 181–187, 2002.

[8] M. F. Modest, *Radiative Heat Transfer*, Academic Press, 2nd edition, 2003.

[9] Y. R. Sivathanu, J. P. Gore, and J. Doliner, "Transient scalar properties of strongly radiating jet flames," *Combustion Science and Technology*, vol. 76, pp. 45–66, 1991.

[10] J. M. Suo-Anttila, T. K. Blanchat, A. J. Ricks, and A. L. Brown, "Characterization of thermal radiation spectra in 2 m pool fires," in *Proceedings of the 32nd International Symposium on Combustion*, pp. 2567–2574, August 2008.